

# Inertial Measurement Unit for On-Machine Diagnostics of Machine Tool Linear Axes

Gregory W. Vogl<sup>1</sup>, M. Alkan Donmez<sup>1</sup>, Andreas Archenti<sup>2</sup>, and Brian A. Weiss<sup>1</sup>

<sup>1</sup>*National Institute of Standards and Technology (NIST), Gaithersburg, Maryland, 20899, USA*

*gregory.vogl@nist.gov*

*alkan.donmez@nist.gov*

*brian.weiss@nist.gov*

<sup>2</sup>*KTH Royal Institute of Technology, Brinellvägen 68, 10044, Stockholm, Sweden*

*archenti@kth.se*

## ABSTRACT

Machine tools degrade during operations, yet knowledge of degradation is elusive; accurately detecting degradation of machines' components such as linear axes is typically a manual and time-consuming process. Thus, manufacturers need automated, efficient, and robust methods to diagnose the condition of their machine tool linear axes with minimal disruptions to production. Towards this end, a method was developed to use data from an inertial measurement unit (IMU) for identification of changes in the translational and angular errors due to axis degradation. The IMU-based method uses data from accelerometers and rate gyroscopes to identify changes in linear and angular errors due to axis degradation. A linear axis testbed, established for the purpose of verification and validation, revealed that the IMU-based method was capable of measuring geometric errors with acceptable test uncertainty ratios. Specifically, comparison of the IMU-based and laser-based results demonstrate that the IMU-based method is capable of detecting micrometer-level and microradian-level degradation of linear axes. Consequently, an IMU was created for application of the IMU-based method on a machine tool as a proof of concept for detection of linear axis error motions. If the data collection and analysis are integrated within a machine controller, the process may be streamlined for the optimization of maintenance activities and scheduling, supporting more intelligent decision-making by manufacturing personnel and the development of self-diagnosing smart machine tools.

## 1. INTRODUCTION

Machine tool linear axes move the cutting tool and workpiece to their desired positions for parts production (Altintas, Verl, Brecher, Uriarte & Pritschow, 2011). A typical machine tool has multiple linear axes, and their accuracies directly impact the quality of manufactured parts. However, over a machine tool's lifetime, various faults lead to performance degradation, lowering accuracy and repeatability (Li, Wang, Lin & Shi, 2014). Typical sources of errors within linear axes are due to pitting, wear, corrosion, and cracks of the system components such as guideways and recirculating balls (Zhou, Mei, Zhang, Jiang & Sun, 2009). As degradation increases, tool-to-workpiece errors increase that eventually may result in a failure and/or a loss of production quality (Uhlmann, Geisert & Hohwieler, 2008). Yet knowledge of degradation is illusive; proper assessment of axis degradation is often a manual, time-consuming, and potentially cost-prohibitive process.

While direct methods for machine tool performance evaluation are well-established (International Organization for Standardization, 2012) and reliable for position-dependent error quantification, such measurements typically interrupt production (Khan & Chen, 2009). An online condition monitoring system for linear axes is needed to help reduce machine downtime, increase productivity and product quality, and improve knowledge about manufacturing processes (Teti, Jemielniak, O'Donnell & Dornfeld, 2010). Efforts to monitor the condition of linear axes components have utilized various sensors, e.g., built-in rotary encoders (Verl, Heisel, Walther & Maier, 2009), current sensors (Uhlmann et al., 2008), and accelerometers (Liao & Lee, 2009; Spiewak, Zaiss & Ludwick, 2013). These attempts at condition monitoring of linear axes had limited success, partly because of the lack of robustness and defined

---

Gregory Vogl et al. This is an open-access article distributed under the terms of the Creative Commons Attribution 3.0 United States License, which permits unrestricted use, distribution, and reproduction in any medium, provided the original author and source are credited.

relationships of signals to axis degradation composed of a wide range of spatial frequencies.

Consequently, efficient quantitative measures are needed to monitor the degradation of linear axes. Recently, accelerometers have been used for dynamic metrology of machine tools (Sato, Nagaoka & Sato, 2015; Smith & Hocken, 2013) and six-degree-of-freedom motion sensors exist within integrated circuit (IC) components (InvenSense Incorporated, 2016). Thus, the use of an inertial measurement unit (IMU) is attractive for on-machine condition monitoring.

One potential solution for online monitoring of linear axis degradation is the use of an IMU (Vogl, Weiss & Donmez, 2015). As seen in the schematic of Figure 1, an IMU is mounted to a moving machine tool component. To diagnose axis degradation, the axis is moved back and forth at various speeds to capture data for different frequency bandwidths. This data is then integrated, filtered, and ‘fused’ to estimate the changes in the 6-degree-of-freedom (DOF) geometric errors of the axis. Because the linear axes are stacked, coordinate transformations may be used with all 6-DOF errors to estimate the errors at the functional point (International Organization for Standardization, 2012). Ideally, data would be collected periodically to track axis degradation with minimal disruptions to production. With robust diagnostics and prognostics algorithms, incipient faults may be detected and future failures may be avoided. In essence, IMU data can be used to help optimize maintenance, production planning, flexibility, and ultimately part quality.

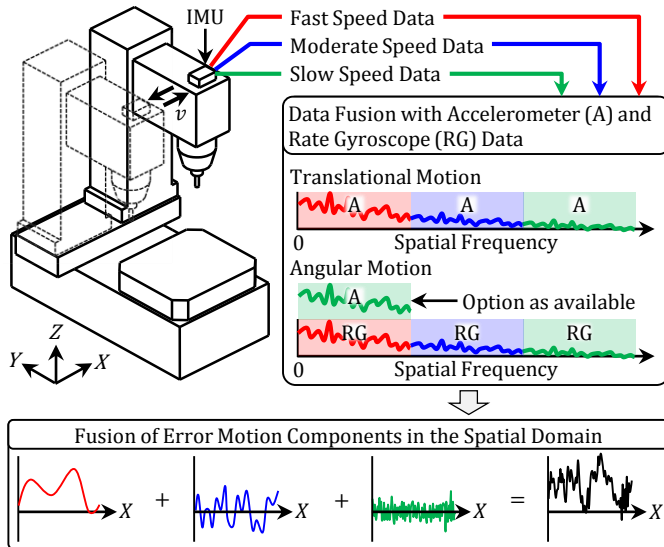


Figure 1. IMU-based method for diagnostics of machine tool performance degradation.

## 2. IMU AND ERROR MOTIONS FOR DIAGNOSTICS

A testbed was designed for evaluation of the IMU-based method. As seen in Figure 2(a), the testbed includes a translation stage, the IMU, a commercial laser-based system for measuring the geometric errors of the axis, and a direct

current (DC) motor with encoder for motion control. While the metrology system measures the motion of the carriage with respect to the base of the linear axis, the carriage-mounted IMU measures the changes in the inertial motion of the carriage. The commercial metrology system measures straightness and angular error motions over the travel length of 0.32 m with standard uncertainties of  $0.7 \mu\text{m}$  and  $3.0 \mu\text{rad}$ , respectively. The laser-based system is used for verification and validation (V&V) of the IMU-based results.

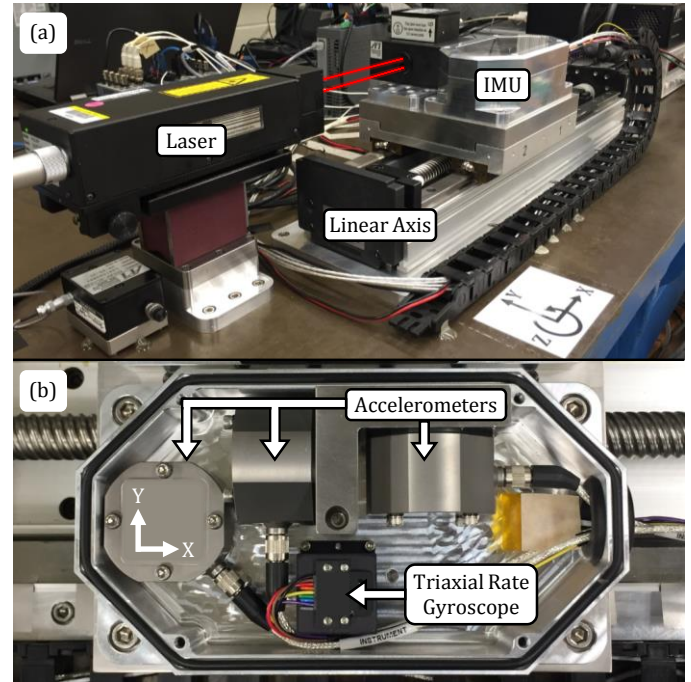


Figure 2. (a) Linear axis testbed and (b) top view of IMU without its lid.

For the detection of both translational and rotational motions, the IMU contains three accelerometers and one triaxial rate gyroscope, as seen in Figure 2(b). Table 1 outlines key specifications of the IMU sensors. Individual sensors were used to obtain sufficiently low noise, despite the larger sensor volume compared to a single 6-DOF IC sensor.

Table 1. Specified properties of sensors used in the IMU

Sensor	Bandwidth <sup>a</sup>	Noise
Accelerometer	0 Hz to 1800 Hz	$4.0 (\mu\text{m/s}^2)/\sqrt{\text{Hz}}$ from 0 Hz to 100 Hz
Rate Gyroscope	0 Hz to 200 Hz	$35 (\mu\text{rad/s})/\sqrt{\text{Hz}}$

<sup>a</sup> frequencies correspond to half-power points, also known as 3 dB points

Consequently, these sensors enable the estimation of 6-DOF motion. A typical machine tool has three linear axes, which means that a total of 18 ( $= 6 \times 3$ ) translational and angular motion errors exist. These errors are major contributors to the position-dependent tool-to-workpiece errors. Figure 3 shows these six errors that change with axis degradation. As the

carriage is positioned along the X axis, it experiences three translational errors from its nominal path: one linear displacement error ( $E_{XX}$ ) in the X-axis direction and two straightness errors ( $E_{YX}$  and  $E_{ZX}$ ) in the Y- and Z-axis directions. The carriage also experiences three angular errors ( $E_{AX}$ ,  $E_{BX}$ , and  $E_{CX}$ ) about the X-, Y-, and Z-axes.

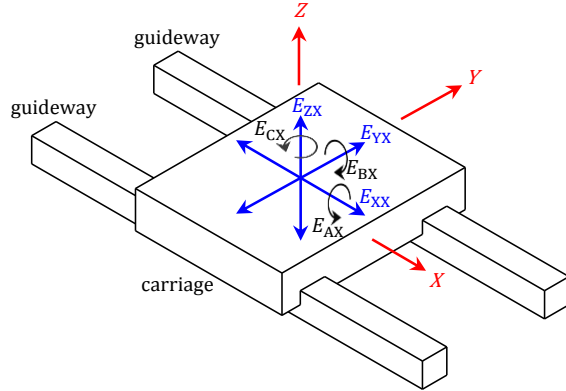


Figure 3. Translational and angular errors of a component commanded to move along a (nominal) straight-line trajectory parallel to the X-axis.

Small levels of degradation of linear axes are expected and allowed, but there are limits specified for axis errors. ISO 10791-2 (International Organization for Standardization, 2001) specifies the tolerances for linear axis errors of vertical machining centers. As shown in Table 2, the acceptable straightness error is limited to  $20\ \mu\text{m}$  and the acceptable angular error is limited to  $60\ \mu\text{rad}$ . A test uncertainty ratio (TUR) of at least 4:1 is deemed to be acceptable, which means that straightness and angular error measurement uncertainties of  $5\ \mu\text{m}$  and  $15\ \mu\text{rad}$ , respectively, are acceptable based on the tolerances outlined in Table 2.

Table 2. Tolerances for linear axis errors of vertical machining centers.

Error	Tolerance*
Straightness	$20\ \mu\text{m}$
Angular (Pitch, Yaw, or Roll)	$60\ \mu\text{rad}$

\* for axes capable of 1 meter of travel, according to ISO 10791-2 (International Organization for Standardization, 2001)

### 3. IMU-BASED METHOD AND GENERAL RESULTS

As outlined in Figure 1, the IMU-based method relies on fusion of data collected at three programmed speeds of the carriage: Fast speed ( $v_1 = 0.5\ \text{m/s}$ ), Moderate speed ( $v_2 = 0.1\ \text{m/s}$ ), and Slow speed ( $v_3 = 0.02\ \text{m/s}$ ). The different speeds allow for sensing of repeatable error motions, composed of low to high spatial frequencies, within different temporal bandwidths. Such a process takes advantage of the enhanced signal-to-noise and lower sensor drift at faster speeds, while taking advantage of the detection of higher spatial frequencies at slower speeds without violating sensor

bandwidths. As seen in Figure 1, matching the spatial cutoff frequencies enables the data fusion, while filtering allows for the attenuation of significant modal excitations, especially resulting from the initial and final accelerations during the Fast speed cycle (Vogl, Donmez & Archenti, 2016).

Figure 4 shows the typical convergence of an estimated straightness error motion and an estimated angular error motion with increasing number of runs for averaging. As seen in Figure 4, 10 runs is usually sufficient for convergence within  $5\ \mu\text{m}$  or  $15\ \mu\text{rad}$ , which means the IMU-based method has the potential to estimate geometric motion errors with a test uncertainty ratio (TUR) of at least 4:1.

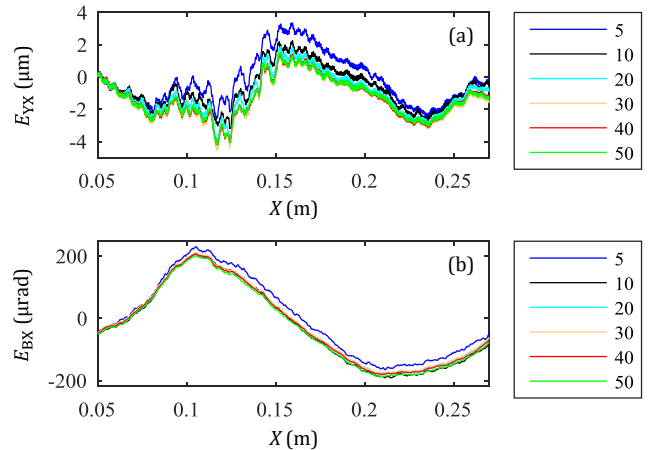


Figure 4. Typical convergence of (a) an estimated straightness error motion (via accelerometer data) and (b) an estimated angular error motion (via rate gyroscope data) with increasing number of runs for averaging (from 5 to 50).

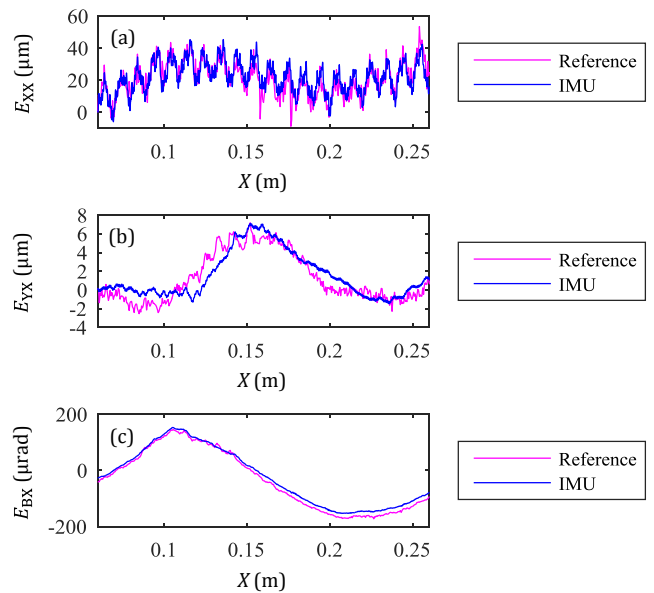


Figure 5. Example of converged (a) linear positioning error motion, (b) straightness error motion, and (c) angular error motion for various sensing methods.

Figure 5 compares the laser-based measurement and IMU-based results; the standard deviations of the differences are  $11\ \mu\text{m}$ ,  $2.3\ \mu\text{m}$ , and  $13\ \mu\text{rad}$  for the linear positioning, straightness, and angular error motions, respectively.

#### 4. TESTBED EXPERIMENTATION

Figure 6(a) shows how a linear axis rail was deformed with shims to simulate low spatial frequency degradations of a machine tool axis. The entire rail was raised with shims so that the center shims could be changed without loosening more than one screw (the center rail screw). Measurements for each case were taken with the reference- and IMU-based systems, resulting in the Y-axis straightness error motions seen in Figure 6(b) and Figure 6(c), respectively. The IMU-based method is able to detect the approximately  $5\ \mu\text{m}$  change in straightness from Case 0 to Case 4, as verified by the reference measurements.

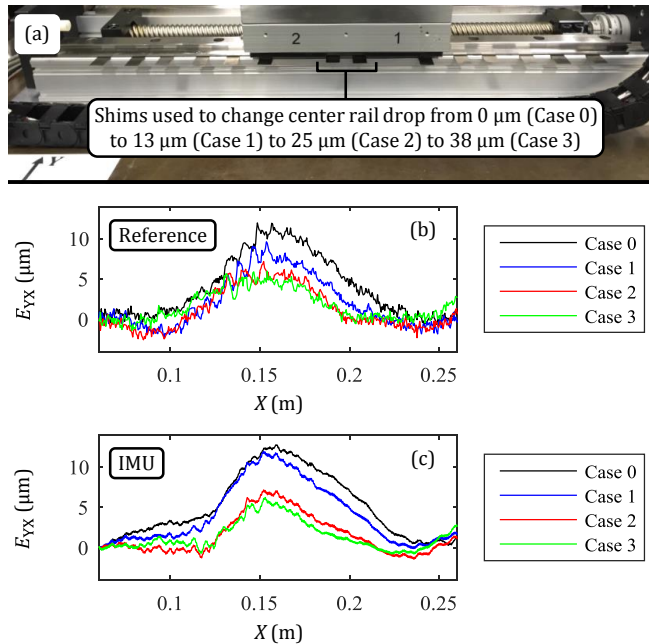


Figure 6. (a) Experimental setup to represent low-frequency degradations of a guideway rail, resulting in changes in straightness error motion ( $E_{YX}$ ) observed by the (b) laser-based reference system and the (c) IMU (data averaged for 50 runs).

One approach for investigating degradation of linear axes is to use filtering to focus on certain sources of errors, such as surface pitting of the rails. Specifically, low-frequency components can be neglected through high-pass filtering. Towards this end, Figure 7(a) shows data smoothed via use of a linear Savitzky-Golay smoothing filter (The MathWorks Incorporated, 2015). The frame size for the Savitzky-Golay filter was chosen to be 2 cm, which is large compared to millimeter-sized defects. Thus, the high-pass filtered data is representative of many defects caused by wear. In Figure 7(a), the error motion ('No filter') is filtered via the Savitzky-

Golay filter to produce low-pass filtered data ('Low-pass'), and the high-pass filtered data ('High-pass') is the complement of the low-pass filtered data; the low-pass and high-pass filtered data sum to yield the unfiltered error motion.

This filtering process can be applied to any linear axis error motion. Figure 7(b) shows typical high-pass filtered data for  $E_{CX}$  for various numbers of runs for averaging (from 5 to 50), where  $hp(E_{CX})$  is the high-pass filtered data of  $E_{CX}$ . As seen in Figure 7(b), convergence for  $hp(E_{CX})$  is achieved to within  $5\ \mu\text{m}$  (TUR = 4) in less than 10 runs for averaging. Furthermore, the high-pass filtered error motion reveals influences from the ball bearings in the trucks. Each ball has a diameter of about 4 mm, which means that each ball rolls on its rail with a ball-passing distance of 12.5 mm (the ball circumference). Figure 7(b) shows how the combined influence of these balls creates a net error motion with significant components dependent upon the ball-passing distance.

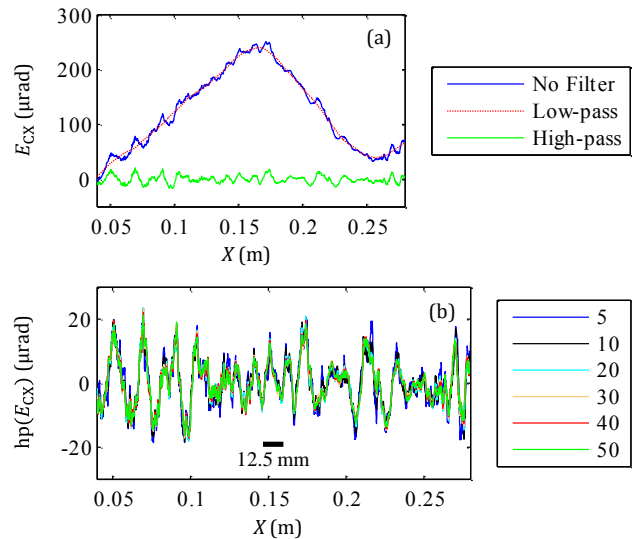


Figure 7. (a) Yaw error motion ( $E_{CX}$ ) separated into low- and high-pass components, and (b) the high-pass component of  $E_{CX}$  for various number of runs for averaging (from 5 to 50).

#### 5. IMU FOR INDUSTRIAL APPLICATION

The IMU seen in Figure 2 was created for testing of the method within the linear axis testbed. For industrial application, the IMU should be physically smaller and more economical while still satisfying the measurement needs.

Consequently, for application on machine tools, an 'industrial IMU' was created that is about 73% smaller than the 'testbed IMU'. As seen in Figure 8, the industrial IMU is about 9 cm long and contains a triaxial accelerometer and a triaxial rate gyroscope. The bandwidths and noise properties of these sensors are seen in Table 3. The rate gyroscope in the industrial IMU is identical to the one used in the testbed IMU. In contrast, the three uniaxial accelerometers seen in Figure



2(b) have been replaced with a triaxial accelerometer seen in Figure 8(b). This change had many advantages: the reduction of space required for acceleration sensors, the elimination of the L-bracket for accelerometer mounting, and a significant reduction of sensor cost. However, the change also had some disadvantages, specifically the reduction of accelerometer bandwidth from 1800 Hz to 500 Hz and the 5-fold increase of accelerometer noise from  $4.0 (\mu\text{m/s}^2)/\sqrt{\text{Hz}}$  to  $20 (\mu\text{m/s}^2)/\sqrt{\text{Hz}}$ .

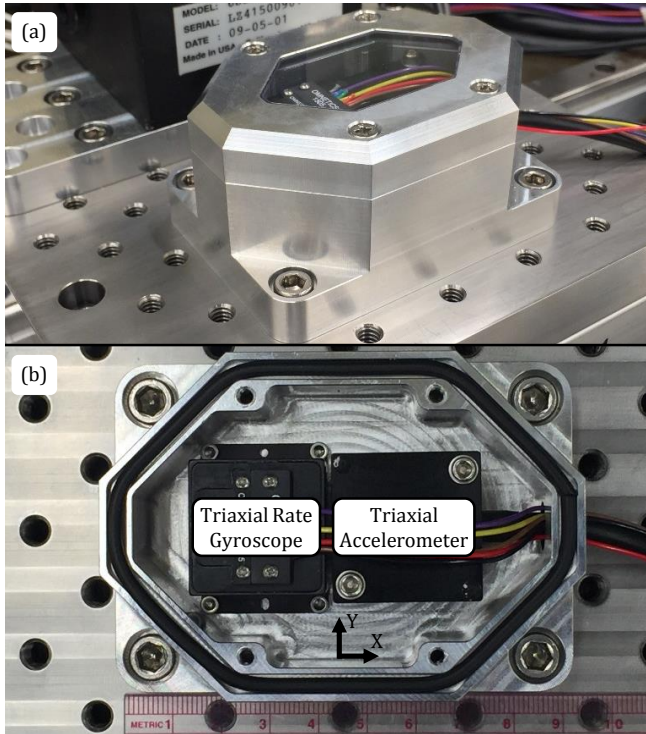


Figure 8. (a) Isometric view of industrial IMU and (b) top view of industrial IMU without its lid.

Table 3. Properties of sensors in industrial IMU

Sensor	Bandwidth <sup>a</sup>	Noise
Accelerometer	0 Hz to 500 Hz	$20 (\mu\text{m/s}^2)/\sqrt{\text{Hz}}$
Rate Gyroscope	0 Hz to 200 Hz	$35 (\mu\text{rad/s})/\sqrt{\text{Hz}}$

<sup>a</sup> frequencies correspond to half-power points, also known as 3 dB points

According to simulations of the data fusion process, the accelerometer used in the industrial IMU will result in approximately twice as much uncertainty in straightness errors as that for the testbed IMU. As seen in Figure 9, the 5-fold increase of accelerometer noise from  $4.0 (\mu\text{m/s}^2)/\sqrt{\text{Hz}}$  (for the testbed IMU) to  $20 (\mu\text{m/s}^2)/\sqrt{\text{Hz}}$  (for the industrial IMU) should result in an approximate 2-fold increase in straightness uncertainty. Figure 9 shows that as the accelerometer noise decreases, the uncertainty decreases to a limit caused by noise of the data acquisition (DAQ) equipment. Experimental data will be collected to confirm the slower rate of convergence for the industrial IMU.

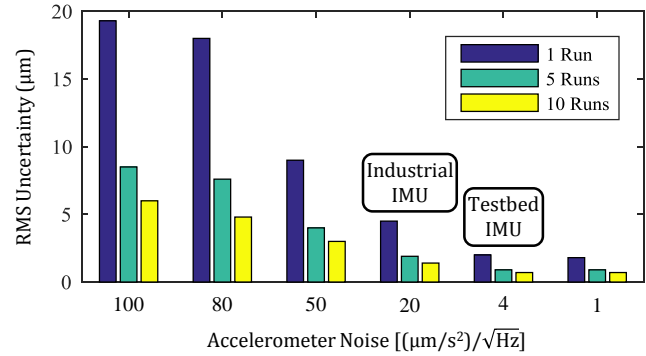


Figure 9. Simulated uncertainty for straightness error motions due to data fusion process with accelerometer noise and data acquisition noise.

## 6. CONCLUSIONS

Manufacturers need efficient and robust methods for diagnosis of machine tool linear axes with minimal disruptions to production. Towards this end, a new IMU-based method was developed for linear axis diagnostics. Measurements from accelerometers and rate gyroscopes are used to identify changes in translational and angular error motions due to axis degradation. Data is fused in the spatial frequency domain via filtering in order to include both low- and high-frequency error motions while excluding significant modal excitations.

A linear testbed was used to verify and validate the IMU-based method through use of a laser-based system for measurement of the geometric axis performance. The IMU-based results typically converge within  $5 \mu\text{m}$  or  $15 \mu\text{rad}$  when using 10 runs for averaging, needed for the estimation of changes in geometric motion errors with test uncertainty ratios of at least 4:1.

Future tests will reveal the effectiveness of the new IMU-based method for on-machine application through use of an 'industrial IMU'. The IMU and the laser-based system (for V&V) will be utilized on various machine tools within the National Institute of Standards and Technology (NIST) Fabrication Technology machine shops. Metrics will be defined based on the collected data to quantify machine tool linear axis degradation, to inform the user of the magnitude and location of wear and any violations of performance tolerances. If the data collection and analysis are integrated within a machine controller, the process may be streamlined for the optimization of maintenance, supporting the development of self-diagnosing smart machine tools. When coupled with existing data exchange and formatting standards, verified and validated data from an 'industrial IMU' could provide manufacturers and machine tool operators with near-real-time equipment health, diagnostic, and prognostic intelligence to significantly enhance asset availability and minimize unscheduled maintenance.

A by-product of this research is that IMU-related experimentation across multiple machines is likely to highlight differences in equipment health between different machine tools. This information can be coupled with equipment performance metrics and quality data (resultant from part inspection) to enable the prediction of future machine performance and part quality based upon current and projected equipment health. Ultimately, this research has the potential to have substantial impact within the manufacturing community.

#### ACKNOWLEDGEMENTS

The authors thank the Fabrication Technology Group (NIST) for their outstanding contributions with the experimental setup.

#### NIST DISCLAIMER

Certain commercial equipment, instruments, or materials are identified in this paper to foster understanding. Such identification does not imply recommendation or endorsement by the National Institute of Standards and Technology, nor does it imply that the materials or equipment identified are necessarily the best available for the purpose.

#### REFERENCES

- Altintas, Y., Verl, A., Brecher, C., Uriarte, L., & Pritschow, G. (2011). Machine tool feed drives. *CIRP Annals - Manufacturing Technology*, vol. 60(2), pp. 779-796. doi: 10.1016/j.cirp.2011.05.010
- International Organization for Standardization (2001). *ISO 10791-2 - test conditions for machining centres – part 2: Geometric tests for machines with vertical spindle or universal heads with vertical primary rotary axis (vertical z-axis)*.
- International Organization for Standardization (2012). *ISO 230-1 - test code for machine tools – part 1: Geometric accuracy of machines operating under no-load or quasi-static conditions*.
- InvenSense Incorporated (2016). *MPU-6050 six-axis (gyro + accelerometer) MEMS MotionTracking™ device*: <https://www.invensense.com/products/motion-tracking/6-axis/mpu-6050/>
- Khan, A. W. & Chen, W. (2009). Calibration of CNC milling machine by direct method. *2008 International Conference on Optical Instruments and Technology: Optoelectronic Measurement Technology and Applications* (p. 716010), November 16-19, 2008, Beijing, China. doi: 10.1117/12.807066
- Li, Y., Wang, X., Lin, J., & Shi, S. (2014). A wavelet bicoherence-based quadratic nonlinearity feature for translational axis condition monitoring. *Sensors*, vol. 14(2), pp. 2071-2088.
- Liao, L. & Lee, J. (2009). A novel method for machine performance degradation assessment based on fixed cycle features test. *Journal of Sound and Vibration*, vol. 326(3–5), pp. 894-908. doi: 10.1016/j.jsv.2009.05.005
- Sato, R., Nagaoka, K., & Sato, T., "Machine motion trajectory measuring device, numerically controlled machine tool, and machine motion trajectory measuring method," USA Patent US9144869 B2, Sep. 29, 2015.
- Smith, K. S. & Hocken, R. J., "Dynamic metrology methods and systems," USA Patent US8401691 B2, Mar. 19, 2013.
- Spiewak, S., Zaiss, C., & Ludwick, S. J. (2013). High accuracy, low-invasive displacement sensor (halids). *ASME 2013 International Mechanical Engineering Congress and Exposition, IMECE 2013* (p. V02AT02A077), November 15-21, 2013, San Diego, CA, United states. doi: 10.1115/IMECE2013-66767
- Teti, R., Jemielniak, K., O'Donnell, G., & Dornfeld, D. (2010). Advanced monitoring of machining operations. *CIRP Annals - Manufacturing Technology*, vol. 59(2), pp. 717-739. doi: 10.1016/j.cirp.2010.05.010
- The MathWorks Incorporated (2015). *Documentation: Sgolayfilt*: <http://www.mathworks.com/help/signal/ref/sgolayfilt.html>
- Uhlmann, E., Geisert, C., & Hohwieler, E. (2008). Monitoring of slowly progressing deterioration of computer numerical control machine axes. *Proceedings of the Institution of Mechanical Engineers, Part B: Journal of Engineering Manufacture*, vol. 222(10), pp. 1213-1219.
- Verl, A., Heisel, U., Walther, M., & Maier, D. (2009). Sensorless automated condition monitoring for the control of the predictive maintenance of machine tools. *CIRP Annals - Manufacturing Technology*, vol. 58(1), pp. 375-378.
- Vogl, G. W., Weiss, B. A., & Donmez, M. A., "A sensor-based method for diagnostics of machine tool linear axes," presented at the Annual Conference of the Prognostics and Health Management Society 2015, Coronado, CA, 2015.
- Vogl, G. W., Donmez, M. A., & Archenti, A. (2016). Diagnostics for geometric performance of machine tool linear axes. *CIRP Annals - Manufacturing Technology*,
- Zhou, Y., Mei, X., Zhang, Y., Jiang, G., & Sun, N. (2009). Current-based feed axis condition monitoring and fault diagnosis. *4th IEEE Conference on Industrial Electronics and Applications, ICIEA 2009* (pp. 1191-1195), May 25-27, 2009, Xi'an, China. doi: 10.1109/ICIEA.2009.5138390

## BIOGRAPHIES



**Dr. Gregory W. Vogl** is a Mechanical Engineer at the National Institute of Standards and Technology (NIST) located in Gaithersburg, Maryland. He received his B.S. (2000), M.S. (2003), and Ph.D. (2006) degrees in Engineering Mechanics from Virginia Tech, Virginia, USA. Currently, Greg is a member of the *Prognostics and Health Management for Smart Manufacturing Systems* (PHM4SMS) project, which seeks to develop a methodology, protocols, and reference datasets to enable robust real-time diagnostics and prognostics for smart manufacturing systems. Previously, he designed, fabricated, and experimented on microelectromechanical systems as a National Research Council Postdoctoral Researcher at NIST. He then joined the Production Systems Group, in which he worked on machine tool metrology and standards development. His interests include machine tool spindle health, diagnostic and prognostic methods, nonlinear dynamics, engineering mechanics, and metrology.



**Dr. Alkan Donmez** is currently the Group Leader of the Production Systems Group as well as the Program Manager for the *Measurement Science for Additive Manufacturing* program in the NIST Engineering Laboratory. He has been with NIST for more than 25 years conducting and supervising research in advanced manufacturing sciences, including machine tool performance modeling and metrology, machining process metrology, as well as the recent efforts in metal-based additive manufacturing. He has actively participated in national and international standard committees, developing machine tool performance testing standards, for more than 20 years. He has published more than 70 technical papers and reports in the area of machine tool metrology and manufacturing sciences. He has received various awards for his technical contributions, including R&D100, Applied Research Award of NIST, and Department of Commerce Silver and Bronze Medals.



**Dr. Andreas Archenti** is conducting research in the field of Precision Engineering and is currently the Research Leader for the Precision Manufacturing and Metrology group at KTH Royal Institute of Technology in Stockholm, Sweden. He received his M.S. (2007) in Mechanical Engineering, and Ph.D. (2011) in Production Engineering focusing on Machine and Process technology from KTH. He is also the Director of the Center for Design and Management of Manufacturing Systems (DMMS) at the KTH. As the Director of DMMS, Andreas is responsible for coordination of activities in research, education, and information dissemination between academia and manufacturing industry. His efforts have

earned him the ABB Alde Nilsson Foundation award for excellence in production research (2011).



**Dr. Brian A. Weiss** has a B.S. in Mechanical Engineering (2000), Professional Masters in Engineering (2003), and Ph.D. in Mechanical Engineering (2012) from the University of Maryland, College Park, Maryland, USA. He is currently the Associate Program Manager of the *Smart Manufacturing Operations Planning and Control* program and the Project Leader of the *Prognostics and Health Management for Smart Manufacturing Systems* project within the NIST Engineering Laboratory. Prior to his leadership roles in the SMOPAC program and the PHM4SMS project, he spent 15 years conducting performance assessments across numerous military and first response technologies including autonomous unmanned ground vehicles; tactical applications operating on Android devices; advanced soldier sensor technologies; free-form, two-way, speech-to-speech translation devices for tactical use; urban search and rescue robots; and bomb disposal robots. His efforts have earned him numerous awards including a Department of Commerce Gold Medal (2013), Silver Medal (2011), Bronze Medals (2004 & 2008), and the Jacob Rabinow Applied Research Award (2006).